Polymer 49 (2008) 3601–3609

Contents lists available at ScienceDirect

Polymer

journal homepage: www.elsevier.com/locate/polymer

Adsorption of star polymers studied by a new numerical mean field theory

Georgios Kritikos, Andreas F. Terzis*

Department of Physics, School of Natural Sciences, University of Patras, GR 26504, Patras, Greece

ARTICLE INFO

Article history:
Received 17 December 2007
Received in revised form 26 May 2008
Accepted 30 May 2008
Available online 4 June 2008

Keywords:
Star polymers
Polymer brush
Self-consistent mean field method

ABSTRACT

We present a systematic theoretical investigation of star-like polymers of various architectures near adsorbing surface, using a new numerical self-consistent mean field theory. The comparison of the experimentally reported adsorption profiles with the predictions of our method shows excellent agreement. The study of the structural properties of the formed brushes indicates that as the number of branches is increased the number of adsorbed polymers is significantly reduced. Mixtures of different kinds of star polymers show interesting behaviors as the more branched polymers try to develop in the outer region of brush. We also estimate the forces obtained when curved surfaces come close as a function of the distance between the surfaces.

1. Introduction

Advanced methods in anionic polymerization have opened up the possibility of creating numerous architectures of star polymers. The star polymers belong to the family of ultra soft colloids and have several industrial applications [1]. The conformational properties of star polymers are significantly different from those of similar linear chains as a result of the influence of the central part of star chains (very high polymer density in this region). Micelles stabilized with the use of polymer brushes, consisting of linear chains, resemble the behavior of this special category of polymeric colloids when the size of the core is much smaller than the size of the chains attached to it. The study of their behavior is an important issue in the scientific area of soft matter.

Although linear polymer brushes have been the subject of many theoretical and experimental studies [2–17], we know less [1,18–25] about the behavior of star polymers when they are forced to form brushes. The experimental study is limited, as their production is not easy especially as the number of branches (functionality) grows. In this work we intend to investigate the behavior of these polymers when they are adsorbed on a solid surface from a solution. Our tool is much cheaper than experimental techniques and can guide the production and research for these polymers. We use a new version of the numerical self-consistence mean field method, which is proved to be efficient for the study of large polymeric systems, where molecular simulations need too much time or even fail to extract results. The new SCF method is compared with experimental data and with results derived with our previous version of nSCF method [26].

In details, we have recently presented a new approach to the numerical self-consistence mean field method (named block numerical self-consistence field (bnSCF) [27]). According to this new version the polymer segments are contained in a 'tube' filled with solvent, which allow the realization of several configurations of the chain. The 'tube' is a chain of cubic sites, set on a cube lattice. The conformation of each chain is developed on a lattice using Kuhn segment, such that the volume of the polymer-chain is the same with the one measured experimentally. As in each point of the lattice the total polymer volume fraction is consisted of more realistic polymer configurations than in previous methods, we can obtain in a more efficient way the contribution to the total volume fraction of each polymer configuration with important statistical weight.

In the following section, we briefly review the bnSCF method and the needed adjustments for the star architectures. Next we compare results from both the theoretical methods (bnSCF and nSCF) with the experimental from Neutron Reflectivity (NR). Moreover, we make predictions for various other star architectures and mixtures. Finally we discuss the results.

2. The block self-consistent field model

2.1. Theoretical formulation

The theoretical formulation was presented thoroughly in our previous work [27]. It is based on an extension of the standard SCF method introduced by Scheutjens et al. [28–32] and improved by Theodorou et al. [33–36]. According to this approach, in the case of

* Corresponding author. Tel./fax: +30 2610 997618.
E-mail address: terzis@physics.upatras.gr (A.F. Terzis).

0032-3861/$ – see front matter © 2008 Elsevier Ltd. All rights reserved.
doi:10.1016/j.polymer.2008.05.042

polymeric solutions, each lattice site is occupied either by both polymer and solvent (polymer-blocks) or entirely by solvent (solvent-blocks). The macromolecular chain placed on the lattice is the block-chain (i.e. a collection of polymer-blocks), which contains the polymer-chain. In this way the polymer-chain is developed in semi-continuum space (see Scheme 1 in Ref. [27]), since the I, L and V conformations of three successive lattice sites, restrict only the block-chain.

We point out that the main advantage of this method is the introduction of various segment conformations depending on the demands of the polymeric system under investigation. In addition, the energy of each block related to the conformation that segments take, can be estimated by more accurate methods and in this way the polymer chains would be more properly weighted. In this study we take advance of the symmetry of the system and instead of the 3-dimensional representation of the polymer-blocks as done in our previous publication [27], we substitute all the segment conformations that are produced by the rotation around the z-axis with only one (see Scheme 1, where we present the possible conformations inside a polymer-block, used in this study). We also neglect possible density fluctuations for the polymer-segment configurations. In this way we reduce the number of combinations for a pair of successive blocks and so the computational time.

The proper description of the system is given again in the context of statistical physics by means of the grand canonical partition function. In order to obtain an expression for the number of molecules $n^{c}_{(i,j)}$ of chain type i of size r^{i}_{j} in conformation c, we minimize the natural logarithm of the maximum term of the partition function with respect to $n^{c}_{(i,j)}$, subject to the full occupancy constraint applied layerwise [26,27]. In general, the nomenclature used in this article is the standard one presented in our previous publications [26,27] and in SCF books and articles [28–36].

In this study we deal with three different chemical species. An ionic group (A), a polymer (B) and a solvent (C). We symbolize the total volume fraction of each specie (Flory segments) in the solution as, ϕ_A, ϕ_B and ϕ_C, respectively. The volume fraction of the block that contains each specie is, ϕ^{b}_{A}, ϕ^{b}_{B} and ϕ^{b}_{C}. The volume fraction (constant) of a specie inside a block is ϕ^{in}_{A}, ϕ^{in}_{B}, $\phi^{in}_{C_A}$ and $\phi^{in}_{C_B}$. We point out that the solvent may be contained inside an A-block, a B-block and a C-block (full with solvent, $\phi^{in}_{C_C} = 1$). If we set zero the interaction (and conformational) energy in the reference state, then for the inhomogeneous state at z layer for sites filled with polymer and solvent, can be written as:

$$\phi_A(z)\chi_{AB}\langle\phi_B(z)\rangle = \phi^{b}_{A}(z)\phi^{in}_{A}\chi_{AB}\phi^{in}_{B}\left\langle\phi^{b}_{B}(z)\right\rangle, \tag{1a}$$

$$\begin{aligned}\phi_A(z)\chi_{AC}\langle\phi_C(z)\rangle = {} & \phi^{b}_{A}(z)\phi^{in}_{A}\chi_{AC}\phi^{in}_{C_A}\left\langle\phi^{b}_{A}(z)\right\rangle \\ & + \phi^{b}_{A}(z)\phi^{in}_{A}\chi_{AC}\phi^{in}_{C_B}\left\langle\phi^{b}_{B}(z)\right\rangle \\ & + \phi^{b}_{A}(z)\phi^{in}_{A}\chi_{AC}\left\langle\phi^{b}_{C}(z)\right\rangle,\end{aligned} \tag{1b}$$

$$\begin{aligned}\phi_B(z)\chi_{BC}\langle\phi_C(z)\rangle = {} & \phi^{b}_{B}(z)\phi^{in}_{B}\chi_{BC}\phi^{in}_{C_B}\left\langle\phi^{b}_{B}(z)\right\rangle \\ & + \phi^{b}_{B}(z)\phi^{in}_{B}\chi_{BC}\phi^{in}_{C_A}\left\langle\phi^{b}_{A}(z)\right\rangle \\ & + \phi^{b}_{B}(z)\phi^{in}_{B}\chi_{AC}\left\langle\phi^{b}_{C}(z)\right\rangle.\end{aligned} \tag{1c}$$

The quantities between the z-dependent variables are the corresponding parameters for the involving lattice block-interactions.

An approach that explains the obtained results is the assumption of second smaller lattice with lattice sites equal to the Flory segment [26,27,33]. The calculation of the interaction energy is achieved using the traditional Flory–Huggins theory. We estimate the interaction parameters on the block-lattice by counting the number of contacts on the second traditional lattice. Of course the second lattice is only a tool to describe the blocks' interaction and does not restrict the possible segment conformations inside the block.

The determination of the critical value for the interaction parameter, where phase separation occurs, is calculated as [26]:

$$\chi_c = \frac{1}{2\left(\overline{\phi}^{in}_{B} - \overline{\phi}^{in}_{B}\overline{\phi}^{in}_{C_B}\right)}. \tag{2}$$

If we call χ^{b} the interaction parameter in our bnSCF method, then the relation with the corresponding parameter χ^{FH} in the traditional nSCF is:

$$\chi^{FH} = 0.5\frac{\chi^{b}}{\chi_c}. \tag{3}$$

According to the mean field self-consistent approximation the segment potential $u_b(z)$ depends only on the kind of the block (b = A, B and C here):

$$u_b(z) = kT\alpha(z) + \frac{\partial(U/L)}{\partial\phi_b(z)} + u^{ref}_{b}. \tag{4}$$

The probability of finding a block in layer z of the interfacial system, relative to finding it in the bulk is given by the segment weighting factor, $G(z) \equiv e^{-u_b(z)/kT}$. Once we know a proper initial condition we can find the statistical weight of the end of an s-segment long chain in layer z, $G(z;s)$. For the forward propagation the recursion relation has the following expression ($s > 1$):

$$G(z, s_{sc}|1) = G(z, s_{sg})\langle G(z, s-1|1)\rangle, \tag{5a}$$

where

$$\begin{aligned}\langle G(z, s-1|1)\rangle \equiv {} & \sum_{s_{sc}=1}^{num_{sc}} \sum_{(s-1)_{sc}=1}^{num_{sc}} \sum_{i=-1}^{+1} \lambda_i \tau_{s_{sc},(s-1)_{sc},i} \\ & \times G(z+i, (s-1)_{sc}|1).\end{aligned} \tag{5b}$$

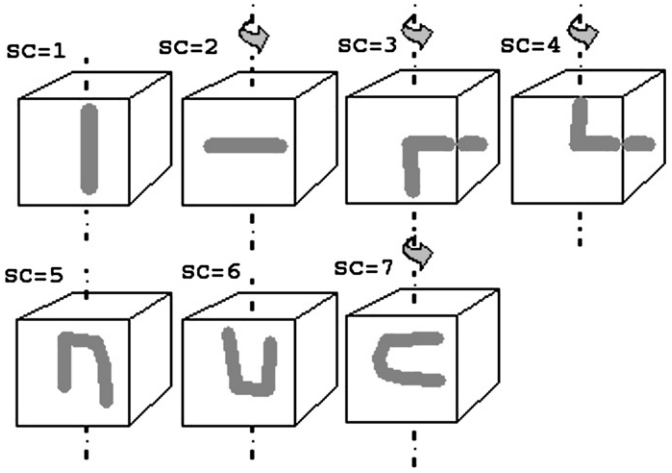

Scheme 1. The seven possible polymer-segment conformations (sc) inside a cube block. Each block is characterized by the side of the cube on which the ends of the segment are put. The blocks are free to rotate around the vertical axis. Hence the different blocks that are produced by this rotation are practically equivalent. The V conformations start and end at the same side of the cube. The conformations sc = 1, 2 belong to the same segment group and have sg = I. All the others segment conformations have sg = L.

For the backward propagation ($s < r$):

$$G(z, s_{sc}|r) = G(z, s_{sg})\langle G(z, s-1|r)\rangle, \tag{6a}$$

where

$$\langle G(z, s-1|r)\rangle \equiv \sum_{s_{sc}=1}^{num_{sc}} \sum_{(s-1)_{sc}=1}^{num_{sc}} \sum_{i=-1}^{+1} \lambda_i \tau_{s_{sc},(s-1)_{sc},i} \times G(z+i, (s-1)_{sc}|r). \tag{6b}$$

Then by means of a composition law we find the volume fractions. For the grafted chains:

$$\phi(z) = \sum_{k=1}^{r^{max}} \sum_{s=1}^{k} \sum_{s_{sc}=1}^{num_{sc}} \phi_{P_{sg}}^{in} \Big\{ G(z, s_{sg})^{-1} \tau_{sg}^{-1} (C_k G(z, s_{sc}|1) \times G(z, s_{sc}|k)) \Big\}, \tag{7}$$

where the polymer segment (P) could be of kind A or B, depending on the structure of the copolymer. The factor $G(z, s_{sg})^{-1}\tau_{sg}^{-1}$ is set in order to take care of the double counting (the Boltzmann factors are estimated in Table 1).

Table 1
Non-zero Boltzmann factors

sc = 1	sc = 2	sc = 3	sc = 4	sc = 5	sc = 6	sc = 7
$\tau_{1,1,-1} = \tau_I$	$\tau_{2,2,0} = \tau_I^*$	$\tau_{3,1,-1} = \tau_L$	$\tau_{4,1,+1} = \tau_L$	$\tau_{5,1,-1} = \tau_L$	$\tau_{6,1,+1} = \tau_L$	$\tau_{7,2,0} = \tau_L^*$
$\tau_{1,1,+1} = \tau_I$	$\tau_{2,3,0} = \tau_I^*$	$\tau_{3,2,0} = \tau_L^*$	$\tau_{4,2,0} = \tau_L^*$	$\tau_{5,4,-1} = \tau_L$	$\tau_{6,3,+1} = \tau_L$	$\tau_{7,3,0} = \tau_L^*$
$\tau_{1,3,+1} = \tau_I$	$\tau_{2,4,0} = \tau_I^*$	$\tau_{3,3,0} = \tau_L^*$	$\tau_{4,3,0} = \tau_L^*$	$\tau_{5,6,-1} = \tau_L$	$\tau_{6,5,+1} = \tau_L$	$\tau_{7,4,0} = \tau_L^*$
$\tau_{1,4,-1} = \tau_I$	$\tau_{2,7,0} = \tau_I^*$	$\tau_{3,4,-1} = \tau_L$	$\tau_{4,3,+1} = \tau_L$			$\tau_{7,7,0} = \tau_L^*$
$\tau_{1,5,+1} = \tau_I$		$\tau_{3,4,0} = \tau_L^*$	$\tau_{4,4,0} = \tau_L^*$			
$\tau_{1,6,-1} = \tau_I$		$\tau_{3,6,-1} = \tau_L$	$\tau_{4,5,+1} = \tau_L$			
		$\tau_{3,7,0} = \tau_L^*$	$\tau_{4,7,0} = \tau_L^*$			

The architecture is such that the adsorbed chain can start with the 1st and 3rd blocks and obtains the factor τ_{sg}. The factors τ_{sg}^* obtain the values $\tau_I^* = 1/4\tau_I$, $\tau_L^* = 1/4\tau_L$. The solvent ($num_{sc}+1$) can follow after every block and from every side of the cube (every λ_i) while the obtained bond energy for this case is τ_{sg}. The three indexes of the factor, τ, are in sequence: the current segment, the previous segment and the side (λ_i) of current site on which the connection is made.

By properly rearranging the order of the summation we get

$$\phi(z) = \sum_{s=1}^{r^{max}} \sum_{s_{sc}=1}^{num_{sc}} \phi_{P_{sg}}^{in} \Big\{ G(z, s_{sg})^{-1} \tau_{sg}^{-1} (G(z, s_{sc}|1)[C_s G(z, s_{sc}|s) + G(z, s_{sc}/\{k \geq s+1\})]) \Big\}, \tag{8}$$

where

$$C_s = \bar{c}\frac{n_s}{n_{total}} \frac{1}{\sum_z G(z, s/1)}, \tag{9}$$

n_s is the number of chains with size s. The total number of chains is n_{total}; $\bar{c}$ is the number of polymer chains per solution volume (related to an average concentration of the total polymer in the solution). We start with an initial value and the final value is adjusted to the requirement of a specific bulk volume fraction.

The adhesion tension between two surfaces (plates) is calculated by the following equation [31,35]:

$$\frac{2(\gamma - \gamma_C)a_s}{kT} = \left(1 - \frac{1}{\bar{r}}\right)\theta^{ex} + \sum_z \ln \frac{\phi_C(z)}{\phi_C^{bulk}} + \chi \sum_z \Big(\phi_P(z)\langle\phi_P(z)\rangle - (\phi_{bulk})^2\Big), \tag{10}$$

where $\theta^{ex} = \sum_z [\phi_P(z) - \phi_{bulk}]$, a_s is the area per site, $\bar{r}$ is the average chain size, γ the surface tension of the pure polymer, γ_C the surface tension of the pure solvent and ϕ_C^{bulk}, ϕ_{bulk} is the solvent and polymer volume fraction in bulk, respectively. In our case the volume fraction of the ionic group is very low (one segment) and has no interaction with the solvent. So the surface tension substantially refers to the block B.

The difference of the free energy for the case of infinity distance between the plates and the case of a specific distance (h) gives the force between the plates ($F_c(h)/R_c$). It is positive for repulsion and negative for attraction and is given by the equation [36]:

$$\frac{F_c(h)}{R_c} = 4\pi([\gamma - \gamma_C] - [\gamma - \gamma_C]_\infty), \tag{11}$$

where R_c is a typical radius, which is much larger than the separation between the plates and much larger than the typical chain dimensions [36].

2.2. Branched chains

The volume fraction of branched chains can be calculated by an extension of the composition law. The formulation was initially derived by Fleer et al. [28]. For example we consider one branch point with three arms. Let us number the segments as shown in Scheme 2. The branch point from which three (or more) branches originate is $s = b$. We use the symbol s_i to denote the ranking number within each branch i, where s_i starts at b and ends at the end point t_i. The branch point participates in all three branches. For a segment s_i ($i = 1, 2, 3$) of the chain we may write:

$$\phi(z, s_i) = CG(z; s_i|t_1, t_2, t_3), \tag{12}$$

where $C = \phi_{bulk}/r$ and $G(z; s_i|t_1, t_2, t_3)$ gives the distribution of segment s_i over the layers z given that the end points of the branches are anywhere in the system.

We choose to start at the branch point. The weight of linear chains starting at t_j and ending at t_k (or conversely) with a segment b on this walk being positioned in layer z may be designed as $G(z; b|t_j, t_k)$. In this way:

$$G(z; b|t_j, t_k) = \frac{1}{G(z)} G(z; b|t_j) G(z; b|t_k). \tag{13}$$

If b is to be the branch point, the linear walk from t_i to b is to end also in z. Therefore:

$$G(z; b|t_1, t_2, t_3) = \frac{1}{G^2(z)} G(z; b|t_i) G(z; b|t_j) G(z; b|t_k), \tag{14}$$

where $i = 1$, 2, or 3 and j and k designate the two remaining branches.

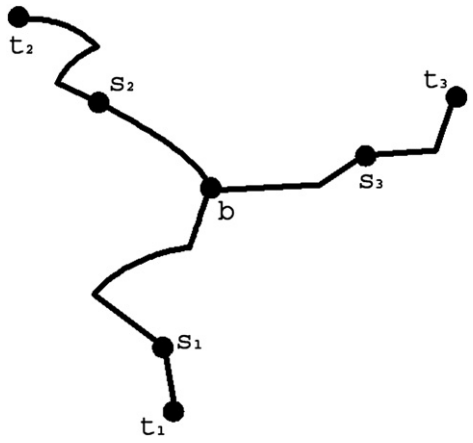

Scheme 2. A star polymer-chain with three branches. The branch point is symbolized as b.

For a segment $s_i \neq b$ on branch i we have

$$G(z;s_i|t_1,t_2,t_3) = \frac{1}{G(z)}G(z;s_i|t_i)G(z;s_i|t_j,t_k). \quad (15)$$

The last factor in Eq. (15) differs from that in Eq. (14) in that s_i is not part of the linear walk t_i, …, t_k. It can be calculated from

$$G(z;s_i+1|t_j,t_k) = G(z)\langle G(z;s_i|t_j,t_k)\rangle. \quad (16)$$

We first apply Eq. (16) for $s_i = b$, for which only Eq. (13) is needed. This gives the distribution for the segment next to b in branch i. We continue successively up to $s_i + 1 = t_i$. Generalization to more arms is straightforward.

2.3. Mapping real polymers onto the lattice

The average polymer volume fraction inside a lattice site (l) is:

$$\overline{\phi}^{\text{in}} = \frac{n_m M_m}{N_A \rho n_b l_b \sin(\theta_b/2)}\frac{1}{l^2}. \quad (17)$$

The number of monomers per block (n_{mpb}) is given by the equation:

$$n_{\text{mpb}} = n_{\text{mpF}}\frac{l}{l_F}, \quad (18)$$

where n_{mpF} is the number of monomers per Flory segment. We mention that the n_{mpb} gives the number of monomers for an isolated block. In every point of the lattice the total volume fraction is given by the overlapping of many different blocks. If we symbolize the number of adsorbed chains per area as σ (chains/nm^2), then the volume fraction of the first polymer segments (adsorbed by surface) is:

$$\phi_{\text{anchor}} = \frac{n_{\text{mpb}}\alpha^3\sigma}{l}\times 10^{-2}, \quad (19)$$

where the volume of the monomer α^3 and the length of the lattice site are given in Å^3 and Å, respectively. If s^2 (nm^2) is the area that occupies one chain then $s^2 = 1/\sigma$ and so through Eq. (19) the inter-anchor spacing (s) is calculated (nm) as:

$$s = 0.1\times\sqrt{\frac{\alpha^3 n_{\text{mpb}}}{l\phi_{\text{anchor}}}}. \quad (20)$$

The bending energies are estimated from the characteristic ratios by matching the mean-square end-to-end distance between a real chain and a chain of correlated Flory segments [26,37].

3. System studied

The experimental results, which we have tried to reproduce with the bnSCF method, refer to a solution that contained three copolymers (nPS$_{70K}$) – X (n = 1, 2, 3), functionalized at one end by a zwitterionic group X = $(CH_3)_2N^+(CH_2)_3SO_3^-$ and attached via short polybutadiene spacers. The first consisted of a dimethylamino end-capped polystyrene (PS) chain (70K molecular weight) and the other two of ω-branched PS chains (70K molecular weight) end-capped with low-molecular-weight ($\overline{M}_n \sim 500$ g/mol) dimethylamino polybutadienes (PB). These macromolecules were synthesized by high-vacuum anionic polymerization techniques [38] and studied with Neutron Reflectivity [39]. The solvent was toluene which is considered a good solvent for PS. Substrates were optically flat quartz slabs. For the zwitterion-surface interaction energy with the surface we use a value of the order of 7–8k_BT estimated in Ref. [8] from force profile experiments on end-adsorbed chains in good solvents and used in the recent experimental and computer simulation study [39]. All solutions are prepared and studied at room temperature [39]. In our theoretical investigation we have also studied other various architectures. In Scheme 3 we present and name all the polymer architectures, presented in this work.

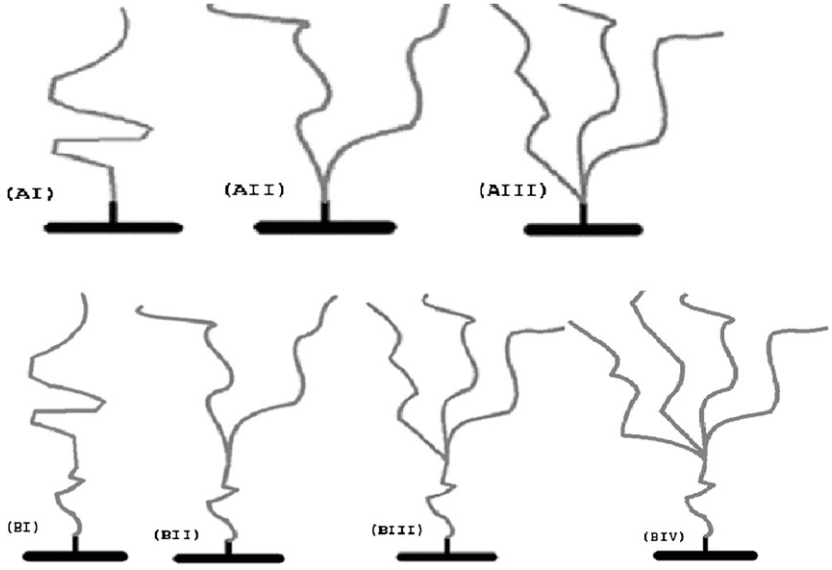

Scheme 3. Schematic representation of the six polymer architectures used in our study. The branches consist of PS chains. Polymers are functionalized at one end by a zwitterionic group (X = $(CH_3)_2N^+(CH_2)_3SO_3^-$, dyed black). The group is attached via short (0.5K) polybutadiene spacer to the rest PS chain. The spacer is considered to have almost the same interaction behavior as the rest of the PS chain. The zwitterionic group together with spacer is represented by 10 PS monomers. In detail we have: (a) a central adsorbing chain of 10 monomers and one branch of 673 monomers, named: AI; (b) an adsorbing chain of 10 monomers and two branches of 673 monomers each, named: AII; (c) an adsorbing chain of 10 monomers and three branches of 673 monomers each, named: AIII; (d) an adsorbing chain of 157 monomers and one branch of 673 monomers, named: BI; (e) an adsorbing chain of 157 monomers and two branches of 673 monomers each, named: BII; (f) an adsorbing chain of 157 monomers and three branches of 673 monomers each, named: BIII; (g) an adsorbing chain of 157 monomers and four branches of 673 monomers each, named: BIV; For cases d–g, the functionality, f is the number of constant size branches plus the adsorbing branch.

The parameter assumed when we applied the bnSCF theoretical method are listed below. The characteristic ratio, C_∞, was chosen as 8.5. For this C_∞, the bending energy is $\varepsilon_L = 0.66 k_B T$. The Kuhn statistical segment for length of the C–C bond 1.54 Å and angle between two consecutive C–C bonds 112° [40] is given as $l_K = 15.79$ Å. The corresponding Flory–Huggins parameters were estimated (A: zwitterions, B: PS/PB, C: toluene and S: surface) as: $\chi_{AB} = 0.0$, $\chi_{AC} = 0.0$, $\chi_{AS} = -48.0$, $\chi_{BC} = 0.3$, $\chi_{BS} = 0$. For this χ_{AS} the corresponding zwitterion-surface interaction energy (for cubic lattice) is $8 k_B T$ (in excellent agreement with the experimental value [39]). The Flory segment was estimated as $l_F = 8.016$ Å, therefore the number of chemical monomers in a Flory segment is 3.143. Also the volume of the monomer is set as 164.08 Å^3, $l = 15.79$ Å and $n_{mpd} = 6.19$. We assume that the polymer segment inside the block occupies the same average volume in all conformations.

In order to achieve a better investigation of the studying system and also test the bnSCF predictions, we have used the nSCF method [26]. For this version the characteristic ratio (C_∞) is equal to 12.0 and the bending energy is taken as $\varepsilon_L = 1.27 k_B T$. The interaction parameters are: $\chi_{AB} = 0.0$, $\chi_{AC} = 0.0$, $\chi_{AS} = -100.0$, $\chi_{BC} = 0.45$, $\chi_{BS} = 0$. The corresponding zwitterion-surface interaction energy (for cubic lattice) is $16.6 k_B T$.

4. Results and discussion

First we present results of our theoretical study (using both bnSCF and nSCF) for the adsorption at constant room temperature as a function of ϕ_{bulk} (see Supplementary data, Fig. S1). The polymer is of type AI (Scheme 3). The graphs show that the predictions of bnSCF reach the "pseudo plateau" at lower values of the ϕ_{bulk}. This is due to the lower value of the χ_{BC}, which was estimated as 0.3 instead of 0.45 with the traditional nSCF. According to theory [28] close to Θ-solvents the adsorption seems to increase without bounds. This prediction is consistent with the experiment, where the value of φ_{bulk} when saturation occurs, is of the order of 10^{-4}. Besides, the experiment [39] characterizes the toluene as a very good solvent for PS. Hence, in order to choose a value for ϕ_{bulk} convenient for both theoretical methods, we choose $\phi_{bulk} = 10^{-3}$.

The very good agreement of the new bnSCF with the experiment is also clearly revealed in the predictions for the volume fraction as function of the distance from the surface. In Fig. 1 we show results of the comparison between predictions from NR experiments and theoretical estimations from both numerical SCF methods. In the linear case (Fig. 1a), the experimental estimation of the adsorption is $\Gamma_{NR} = 3.40$ mg/m^2. The theoretical predictions are $\Gamma_{bnSCF} = 3.80$ mg/m^2 and $\Gamma_{nSCF} = 3.99$ mg/m^2. For case presented in Fig. 1b we have: $\Gamma_{NR} = 2.40$ mg/m^2, $\Gamma_{bnSCF} = 1.96$ mg/m^2 and $\Gamma_{nSCF} = 1.80$ mg/m^2. Also in case of three branches (Fig. 1c), $\Gamma_{NR} = 1.40$ mg/m^2, $\Gamma_{bnSCF} = 1.33$ mg/m^2 and $\Gamma_{nSCF} = 1.00$ mg/m^2. As a conclusion the bnSCF follows better the experimental data as the number of branches increases.

In Table 2 we compare predictions of our method (bnSCF) and experimental results from NR. Although our theoretical predictions indicate higher values for inter-anchor spacing, the relative increment as a function of the number of branches is in very good agreement. The experimental results give: $s_{AII}/s_{AI} = 1.7$, $s_{AIII}/s_{AII} = 1.6$ and $s_{AIII}/s_{AI} = 2.7$. While the theoretical results give: $s_{AII}/s_{AI} = 1.9$, $s_{AIII}/s_{AII} = 1.5$ and $s_{AIII}/s_{AI} = 2.8$. As the volume fraction profile from NR does not show accurate results on the surface, we could assume that the results for the inter-anchor spacing indicate higher σ and so higher volume fraction (on the surface-first layer) compared to the predictions from bnSCF. For this reason we conclude that a smaller depletion layer, compared to the one that the numerical methods give, would be closer to reality.

In this study we have avoided the use of the parameter δ, which is a measure of the deviation from the random walk growth [26] and allows a diminishing of the depletion layer with the chains placed on the surface more like "grafted sticks". The use of the disturbed walk for the region of high polymer concentration gives increased adsorption (σ), especially for the linear chains (not shown). This is due to the change in the shape, from "compressed mushroom" to more uniformly elongated configurations (Scheme 2 in Ref. [26]). We point that it is different to approach the region of

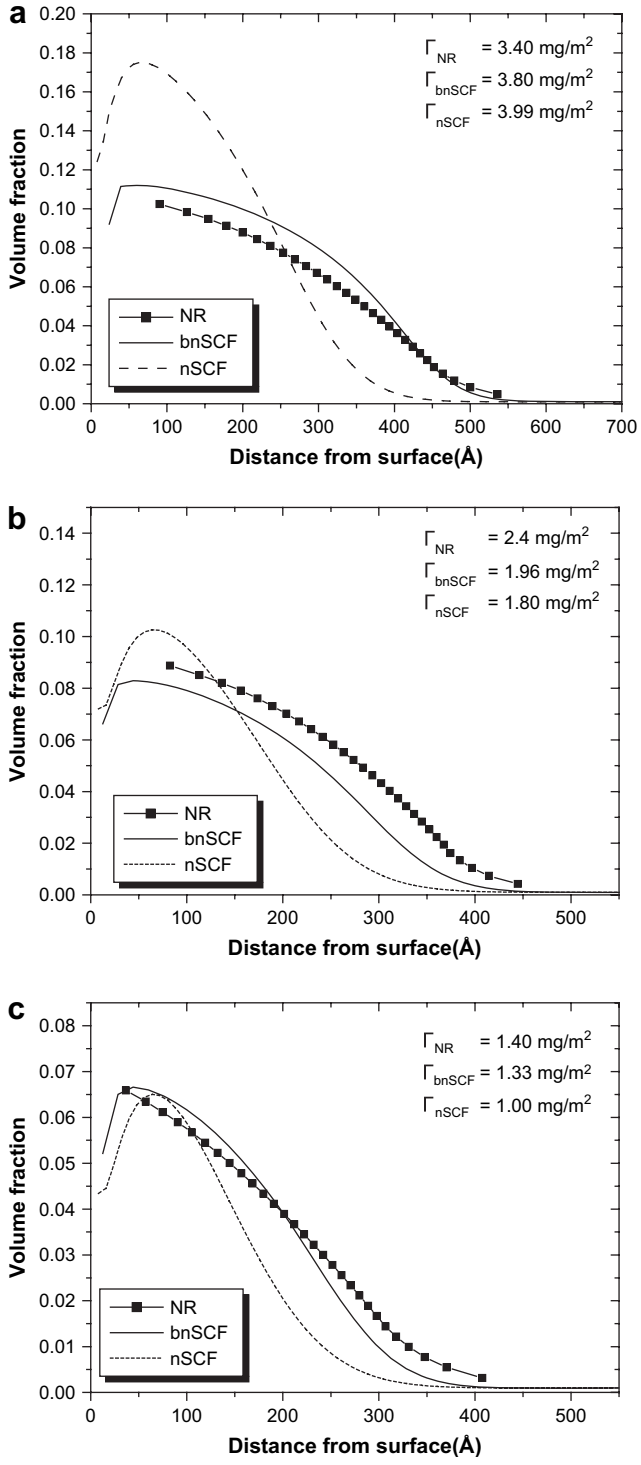

Fig. 1. Volume fraction profiles as a function of the distance from the surface. The symbols depict the NR experimental results; the solid curves – the predictions of bnSCF model and the dash curves – the prediction of nSCF model. The systems studied are: (a) Linear polymers with one PS branch, AI; (b) star polymers with two PS branches, AII; (c) star polymers with three PS branches, AIII.

Table 2
Inter-anchor spacing calculated from Neutron Reflectivity measurements [39] and from our theoretical bnSCF method

Type of star polymer	s (nm) from NR	s (nm) from bnSCF
AI	5.8	18.2
AII	9.8	34.4
AIII	15.8	50.6

high stretching by accepting a third regime in adsorption kinetics [41], as done with the acceptance of chains conformations governed by the disturbed walk, compared to the approach of only two regimes. We suggest that according to the first approach when the chains overlapping exceeds a curtain value [26] the spatial gradient in concentration, due to depletion layer, causes the polymers to flatten near the surface in order to reduce the concentration gradient-depletion layer. As the existence of depletion is proven by both theoretical and experimental techniques [42], it is reasonable to assume that the constantly moving (changing configurations) tethered chains would prefer conformations that are guided by the effort to reduce polymer contacts while at the same time fill this gap. But these conformations cost a lot as far as the entropy is concerned. If the adsorbing energy is not high enough it causes the chains to desorb, while others take their place in order to retain a constant σ. In this way a dynamic equilibrium is established with the desorption rate being small [43]. If the adsorbing energy is very high the chains manage to make more room for others to come. In the third region the results from the bnSCF (Fig. 16 in Ref. [26]) showed a little shrinkage due to the introduction of the parameter δ. Of course elongation that would push the chains reach almost their full lengths is only succeeded for very high σ ("high dense"), while in our previous work we've studied "moderate dense" brushes [44]. But even in this case it was detectable through δ a third region in the adsorption where "high dense" brushes can occur and saturation is reached with the requirement of very high adsorption energy.

On the other hand the increase in the number of branches is a counter factor that favors more parallel to the surface orientations that would increase the sphericity (hemisphericity) of the star polymer [1]. The parameter δ reduces the influence of the entropic factor in the chain shape and describes the energy cost for an adsorbed chain to penetrate vertically the polymer brush, for cases where the chains configurations are governed by the effort to reduce the contact (high σ and adsorption energy). While the increase of functionality, f, makes the entropic factor more determinant leading to stiff spherical particles [1], in the limit of high f that prevent the "soft contact" and strait placement between neighbouring adsorbed polymers. So for high functionality ($f > 2$) where, as will be shown next, the star polymers are stiff and succeed low adsorption, it is clear that we do not have to use δ and in this way we reduce the number of parameters needed to describe the system. We may say that highly branched star polymers (high f) and dense linear polymer brushes (high σ) resemble a "porcupine" with intense resistance to compression [1].

In Fig. 2 we present the volume fraction of the free ends of the systems presented above. Both theoretical methods show that as the number of branches increase, the free ends are distributed closer to the surface (the results of the nSCF method are not shown). This is mainly caused because the more branched polymers exhibit lower adsorption and so the elongation of the brush is less intense compared to linear polymers. So due to entropic reason the more branched polymers need more space to develop and this forces the free ends to cover the whole brush area (not just the outer region).

This is supported by results related to the orientation perpendicular to the surface. In Fig. 3 is shown the total volume fraction of

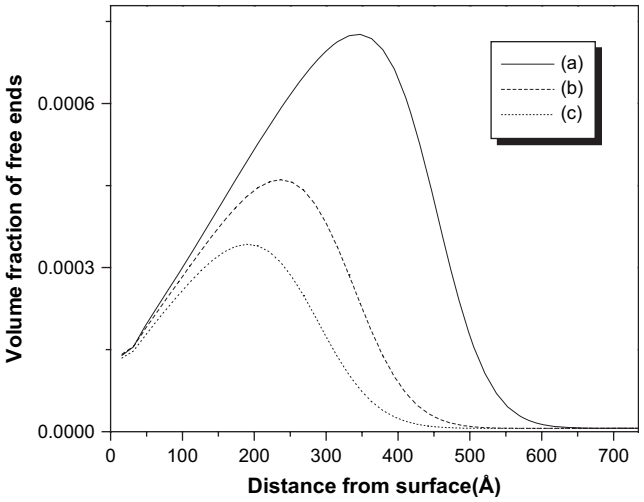

Fig. 2. Volume fraction profiles of the free ends for the polymers studied in Fig. 1. For star polymers the free ends correspond to the free ends of every free branch. Results achieved applying the bnSCF model.

the blocks that allow the chain growth in adjacent layers ($\phi_{sc=1} + 0.5\phi_{sc=3} + 0.5\phi_{sc=4} + \phi_{sc=5} + \phi_{sc=6}$) divided with the value of the same quantity in bulk (far from the surface). We observe that as the number of branches increase the elongation of the chain is reduced and so the orientation is perpendicular to the surface. The predictions of the nSCF method are analogue (not shown).

When two surfaces (capable to adsorb polymers) come closer, the free energy of interaction for the polymer–solvent system changes. If the difference ($\gamma - \gamma_C$) is negative, it is an indication of adsorption. Values greater or equal to zero characterize depletion. In Fig. 4a (polymer of type AI) we observe adsorption according to bnSCF until ~130 Å and according to nSCF until ~280 Å. In the case depicted in Fig. 4b (AII) the bnSCF predicts adsorption until ~145 Å and the nSCF until ~280 Å. While in the case depicted in Fig. 4c (AIII), the bnSCF estimates adsorption until ~145 Å and the nSCF until ~280 Å. For shorter distances we observe depletion due to entropic restrictions.

The reason for both polymers AII and AIII leaving the gap between the surfaces at almost the same distance is that the branches in both cases tend to have almost the same orientation perpendicular to the surface (Fig. 3). The bnSCF method predicts shorter distances for which adsorption is obtained. This is due to the

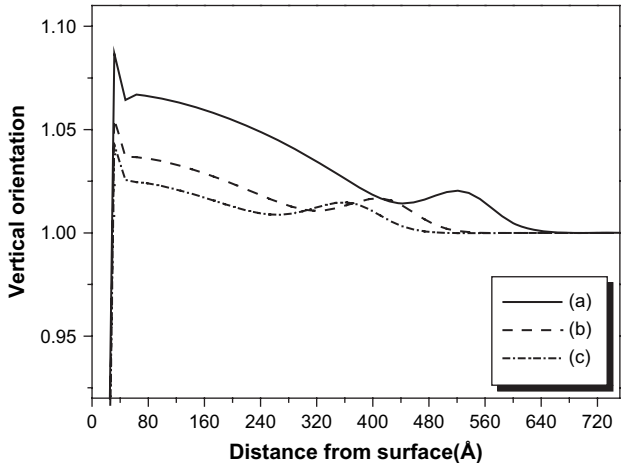

Fig. 3. Orientation perpendicular to the surface (see text) as a function of the distance from the surface, for the polymer architectures studied in Figs. 1 and 2.

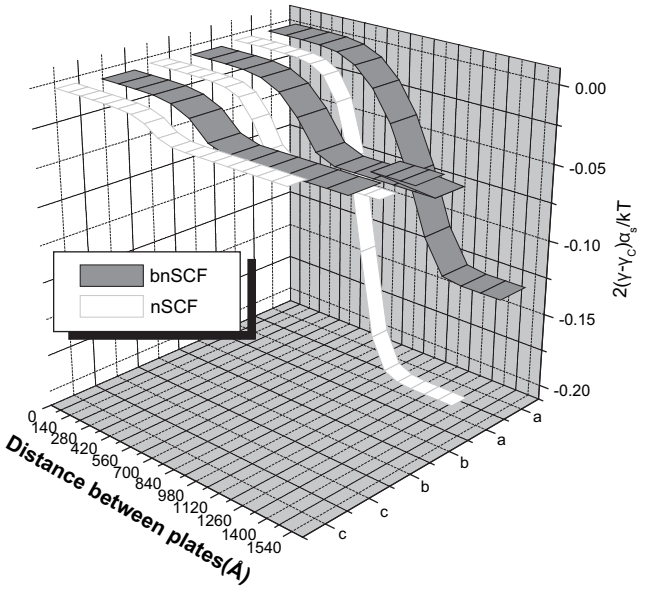

Fig. 4. Plots of the difference of the surface tension (between polymer and solvent) as a function of the distance between the two plates. For adsorbing polymer this difference is negative. We observe that at small distances (in equilibrium) the polymer is not adsorbed. The three cases correspond to the three polymer architectures discussed in Fig. 1. The white curves correspond to the nSCF, while the gray to the new bnSCF.

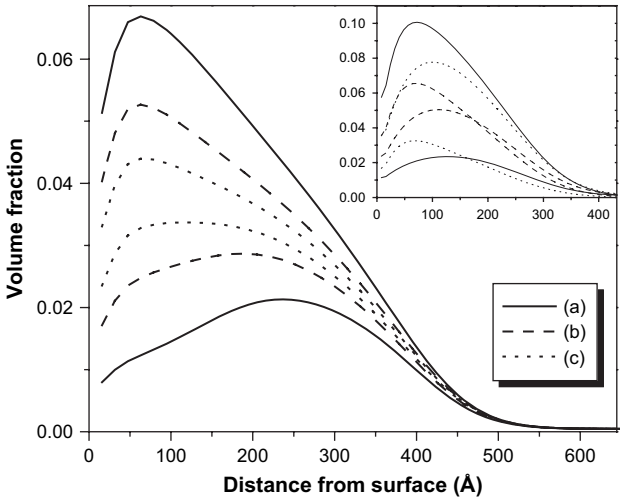

Fig. 5. Study using the bnSCF model of star polymer mixtures of two kinds of PS chains (consisted of types BI and BII polymer). We present the volume fraction profiles as a function of the distance from the surface. The systems studied are: (a) 75% BI and 25% BII (solid curve); (b) 50% BI and 50% BII (dashed curve); (c) 25% BI and 75% BII (dotted curve). In the inset we present the predictions of the nSCF model.

introduction of different chain configurations compared to nSCF method. In this way we give more weight to different conformations and calculate different changes in the entropy (product of all λ_i) [27], which is proved to be more realistic.

Then we have estimated the forces obtained while the two surfaces come closer (see Supplementary data, Fig. S2), for the polymer cases AI and AIII. The force calculated by the bnSCF method for the case AIII is higher compared to nSCF because the adsorption is higher and so the brush resists more to the pressure of the approaching surface. The comparison with typical experiments [8] shows important variations for short distances. This happens because according to the theoretical approach the system is in equilibrium and in this condition the polymers leave the gap between the surfaces. We may assume that a fast approach of the two surfaces would not ensure the irreversibility of the procedure and could trap some polymers and make them respond in an elastic way. Also a higher value in the obtained forces could be succeeded for higher values of the quantity $[\gamma - \gamma_C]_\infty$. This could happen by choosing higher ($>8k_BT$) zwitterion–surface interaction energy. In this way chains that would be still adsorbed by the surfaces even for low distances (100–200 Å) could resist giving another slope to force–distance profiles (as typical experiments indicate).

Next we investigate the behavior of other star architectures with greater functionality, where the constant sized branches are attached to the surface by a shorter (comparing to the other branches) branch ending at a zwitterion. This adsorbing chain that carries the X-group, has 157 monomers, almost sixteen times longer than the central chain of the A-system (see Scheme 3). In this case (B-systems) in the estimation of the functionality, *f*, we include the central strongly (as it carries the X-group) adsorbing branch. Obviously, we should consider the special behavior of this branch. Actually, we investigate mixtures of two B-type polymers. As in the study of A-polymers, the total polymer volume fraction very far from the surface (bulk) is set at 10^{-3}. Each mixture is characterized by the percentage of its species of the mixture in the bulk. In Fig. 5 we show results for the volume fraction for a mixture of linear (BI) and two-branch star polymers (BII). In general the polymers with two branches tend to develop in the outer region of the brush. In case of low percentage (25%) of the BII this tendency is more pronounced. As the percentage of the BII polymer increases the chains need more space to develop and so they are distributed more broadly. Very similar results reveal the study of a mixture of star polymers with two BII and three BIII branches. Again the polymer with more branches BIII tends to develop in the outer region of the brush, once the percentage in the mixture is low (25%). As the percentage increases, the polymer BIII spreads more uniformly in order to gain space.

In Fig. 6 we plot the total volume fractions of the mixture (i.e. the volume fraction of both species of the mixture). We clearly see that the total volume fraction of the mixture does not show two 'parabolic' regions as in the case of bimodal linear polymers [26,34].

We also present predictions for a mixture consisting of a linear (BI) and a highly branched (BIV) polymer architectures (Fig. 7). In this case we observe similar behavior as the one found in system BI–BII but now in a more intense way. The tendency of the linear chains to develop in the inner regions and the branched in the outer region of the brush is very characteristic, especially for low percentage of the star polymer. When the percentage of the linear chains increases the star polymers also spread closer to the surface.

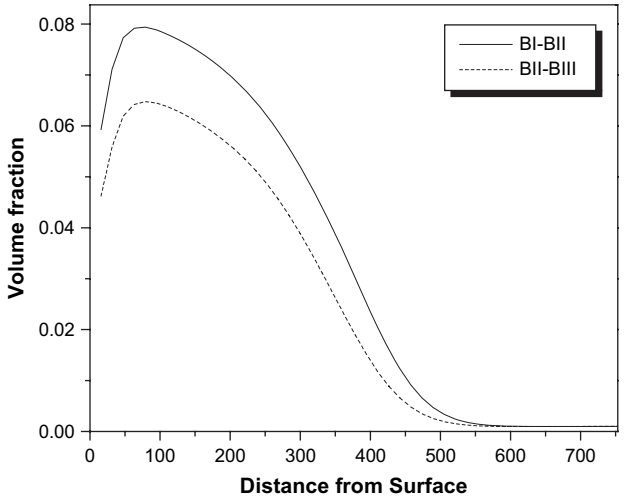

Fig. 6. Total volume fraction profiles as a function of the distance from the surface, for two kinds of mixtures: (i) 75% BI and 25% BII (solid curve) and (ii) 75% BII and 25% BIII (dotted curve). The predictions are from the bnSCF model.

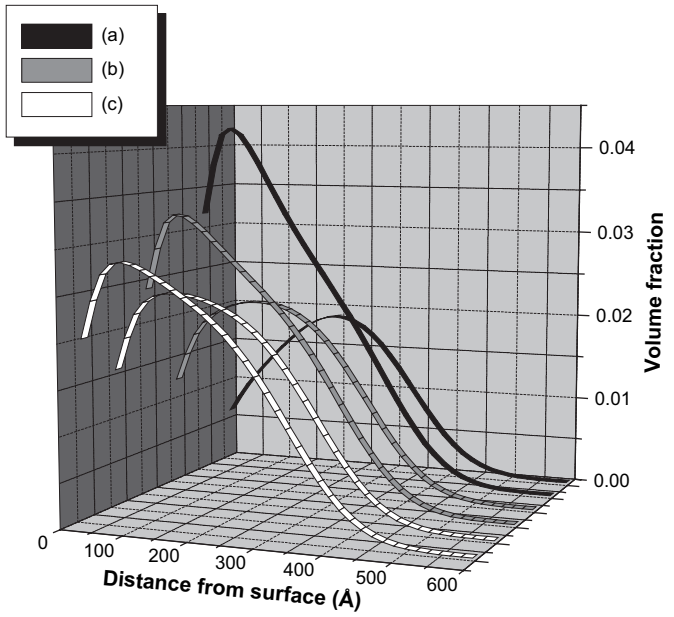

Fig. 7. Volume fraction profiles as a function of the distance from the surface, for mixtures of PS polymer of types BI and BIV. The predictions are from bnSCF. The systems studied are: (a) 75% BI and 25% BIV (black curve); (b) 50% BI and 50% BIV (gray curve); (c) 25% BI and 75% BIV (white curve).

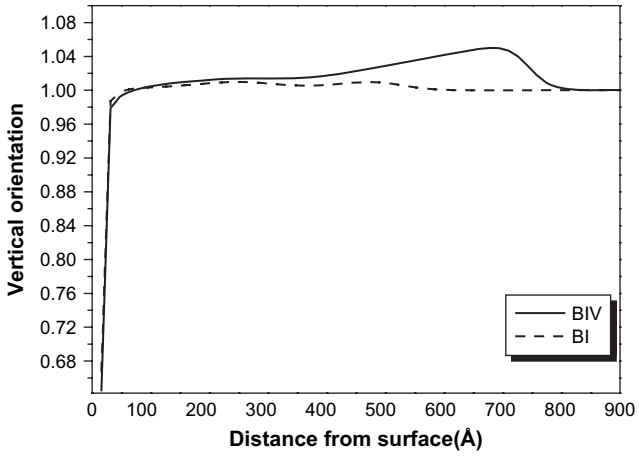

Fig. 8. Vertical Orientation to the surface as a function of the distance from the surface, for the polymer architectures studied in Fig. 7(a).

According to both theoretical methods the variation in the total volume fraction in the three cases (a, b and c) studied in Figs. 5 and 7, is not significant. This could be explained by the fact that the chains tend to arrange themselves in such a way (shrink or elongate) that the maximum adsorption is accomplished by the minimum reduction in the entropy of the system.

A more detail view of the chains' arrangement in the last example (BI–BIV) may be obtained by the volume fraction of the free ends (Supplementary data, Fig. S3). It is confirmed that the more branched polymers tend to develop in the outer region. Both nSCF versions agree that the volume fraction of the free ends for the linear polymers reaches the maximum closer to the surface compared to branched polymer (BIV). Moreover, in cases where the more branched polymers have significant percentage in the solution (Supplementary data, Fig. S3c) their free ends are shown to cover almost the whole brush region. In all cases (a, b and c) the linear chains seem to take almost undisturbed conformations filling the gap under the "umbrella" of the branched chains. Finally we found that the orientation of the BIV polymer is independent of the percentage of the linear chain. The results shown in Fig. 8 for the case (a) are also representative for the other two cases. This outcome confirms the speculation that star polymers, as f increases, behave like stiff spherical particles [1].

The forces obtained as two surfaces covered with polymer (system BI–BIV) approach each other are of the order of 10^{-3} μN/m (see Supplementary data, Fig. S4) for all cases (different percentages). The reason for this behavior is that the reaction to compression is mainly due to the star polymer (BIV) which has the same compressibility in all cases. Besides, the force is calculated through the adhesion tension which depends on the total volume fraction. As the total volume fraction in all cases (Fig. 7) is almost the same this has as a consequence the force to remain almost invariable.

Moreover, in the present study it was estimated that for mixtures where star polymers with high f are majority (75%), while f varies from 3 to 5, the adsorption amount tends to a plateau value (1.1 mg/m^2, 0.8 mg/m^2 and 0.7 mg/m^2, respectively). This supports the idea that polymers with functionality greater than 2 behave like stiff particles [1]. Moreover, we have found that the branches dimensions are not significantly decreased compared to the extension of the adsorbing branch [45].

To our knowledge there is no theoretical or computational investigation of brush systems as those studied in this article. The only systems that have some similarities with those studied by us are the star polymer brushes studied using lattice Monte Carlo simulations by Sikorski et al. [24,45,46] and by Zhang and Xu and Chen et al. using the bond-fluctuation MC method [23]. The major difference between the systems studied there and the ones studied here, has to do with the X-end group which is very short element that has a very high sticking energy with the surface. In addition Sikorski's works [24,45,46] have treated only single chains (infinite dilute systems). However, in order to test the validity of our bnSCF method, we have simulated systems similar to those investigated in Refs. [23,24,45,46], and we have found that our predictions for the static properties of these star polymers are in qualitative agreement with their results.

5. Conclusions

The equilibrium properties of polymer brushes formed by center adsorbed star polymers on solid surfaces were investigated using a new numerical self-consistent mean field theory. By the systematic theoretical investigation of these star-like copolymers of various architectures interesting features are revealed related to their special architecture.

The comparison of the experimentally reported adsorption profiles with the predictions of our method shows excellent agreement. The study of the structural properties of the formed brushes indicates that as the number of branches is increased the number of adsorbed polymers is significantly reduced. Mixtures of different kinds of star polymers show interesting behaviors as the more branched polymers try to develop in the outer region of brush. We also estimate the forces obtained when surfaces come closer as a function of the distance between the surfaces.

In general the improved SCF numerical method is proved to be adequate for quantitatively reproducing the main features of the system under study.

The future plans with these 'ultra soft colloids' will include the systematic study of other more complicated structures.

Acknowledgements

This work was supported by the Greek Secreteriat for Research and Technology (GGET) by a grant (PENED 03ED856).

Appendix. Supplementary data

Fig. S1. Plot of the adsorption (mg/m^2) as a function of the polymer volume fraction in the bulk, for the AI polymer.

Fig. S2. Force–distance profiles between surfaces for linear polymer (AI) and for polymer with three branches (AIII). The system is in equilibrium. Results achieved by applying the bnSCF model.

Fig. S3. Volume fraction of the free ends of the systems studied in Fig. 7. The solid curves describe the prediction of bnSCF model and the dashed curves, the prediction of nSCF model.

Fig. S4. Force–distance profiles between surfaces for the polymeric system of Fig. 7. The system is in equilibrium. Results achieved by applying the bnSCF model.

Supplementary data associated with this article can be found in the online version, at doi:10.1016/j.polymer.2008.05.042.

References

[1] Likos CN. Soft Matter 2006;2:478.
[2] Alexander SJ. J Phys (Paris) 1976;38:977.
[3] DeGennes P-G. Macromolecules 1980;13:1069;
DeGennes P-G. Scaling concepts in polymer physics. Cornell University Press; 1979.
[4] Milner ST, Witten TA, Cates ME. Macromolecules 1988;21:2610;
Milner ST. Science 1991;252:905.
[5] Harpelin A, Tirrell M, Lodge TP. Adv Polym Sci 1992;100:31.
[6] Granick S. Polymers in confined environments. Berlin: Springer; 1999.
[7] Taunton HJ, Toprakcioglu C, Fetters LJ, Klein J. Nature 1988;332:712.
[8] Taunton HJ, Toprakcioglu C, Fetters LJ, Klein J. Macromolecules 1990;23:571.
[9] Klein J, Perahia D, Warburg S. Nature 1991;352:143.
[10] Tirrell M, Patel S, Hadziioannou G. Proc Natl Acad Sci USA 1987;84:4725.
[11] Ansarifar MA, Luckham PF. Polymer 1988;29:329.
[12] Taunton HJ, Toprakcioglu C, Klein J. Macromolecules 1988;21:3333;
Dorgan JR, Stamm M, Toprakcioglu C, Jerome R, Fetters LJ. Macromolecules 1993;26:5321.
[13] Cosgrove T, Heath T, van Lent B, Leermakers F, Scheutjens JM. Macromolecules 1988;20:1692.
[14] Patel SS, Tirrell M. Ann Rev Phys Chem 1989;40:597.
[15] Jones RAL, Richards RW. Polymers at surfaces and interfaces. Cambridge: Cambridge University Press; 1999.
[16] Retsos H, Terzis AF, Anastadiadis SH, Anastasopoulos DL, Toprakcioglu C, Theodorou DN, et al. Macromolecules 2002;35:1116.
[17] Mattice WL, Suter UW. Conformational theory of large molecules. New York: John Wiley & Sons; 1994.
[18] Kosmas MK. Macromolecules 1990;23:2061.
[19] Carignano MA, Szleifer I. Macromolecules 1994;27:702.
[20] Cherepanova TA, Stekolnikov AV. Mol Phys 1994;83:1065.
[21] Shida K, Ohno K, Kimura M, Kawazoe Y. J Chem Phys 1996;105:8929.
[22] Cui Shi-Min, Chen Zhen Yu. Phys Rev E 1997;55:1660.
[23] Zhang L, Xu Y. Eur Polym J 2000;36:841;
Chen J, Zhang L, Cheng J. J Chem Phys 2004;121:11481.
[24] Sikorski A. Macromol Theory Simul 2001;10:38;
Sikorski A. Macromol Theory Simul 2002;11:359;
Sikorski A. Macromol Theory Simul 2003;12:325.
[25] Glynos E, Chremos A, Petekidis G, Camp PJ, Koutsos V. Macromolecules 2007;40:6947.
[26] Kritikos G, Terzis AF. Polymer 2005;46:8355.
[27] Kritikos G, Terzis AF. Polymer 2007;48:638.
[28] Fleer GJ, Cohen Stuart MA, Scheutjens JM, Cosgrove T, Vincent B. Polymers at interfaces. Cambridge: Chapman and Hall; 1993.
[29] Scheutjens JM, Fleer GJ. J Phys Chem 1979;83:1619.
[30] Scheutjens JM, Fleer GJ. J Phys Chem 1980;84:178.
[31] Scheutjens JM, Fleer GJ. Macromolecules 1985;18:1882.
[32] Evers OA, Scheutjens JM, Fleer GJ. Macromolecules 1990;23:5221.
[33] Fischel LB, Theodorou DN. J Chem Soc Faraday Trans 1995;91:2381.
[34] Terzis AF, Theodorou DN, Stroeks A. Macromolecules 2000;31:1312;
Terzis AF. Polymer 2002;43:2444.
[35] Theodorou DN. Macromolecules 1988;21:1400.
[36] Theodorou DN. Macromolecules 1989;22:4589.
[37] Wijmans CM, Leermakers FAM, Fleer GJ. J Chem Phys 1994;101:8214.
[38] Sakellariou G, Pispas S, Hadjichristidis N. Macromol Chem Phys 2003;204:146.
[39] Hiotelis I, Koutsioubas A, Spiliopoulos N, Anastasopoulos D, Vradis A, Toprakcioglou C, et al. Macromolecules, in press.
[40] Mark JE. Physical properties of polymers handbook. WoodBury, New York: American Institute of Physics Press; 1996;
Brandrup J, Immergut EH. Polymer handbook. 3rd ed. New York: John Wiley & Sons; 1989.
[41] Penn LS, Huang H, Sindkhedkar MD, Rankin SE, Chittenden K. Macromolecules 2002;35:7054.
[42] Kent MS, Lee LT, Factor BJ, Rondelez F, Smith GS. J Chem Phys 1995;103:2320.
[43] Motschamann H, Stamm M, Toprakcioglu C. Macromolecules 1991;3681:24.
[44] Yamamoto S, Ejaz M, Tsujii Y, Fukuda T. Macromolecules 2000;33:5608.
[45] Romiszowski P, Sikorski A. J Chem Inf Comput Sci 2004;44:393.
[46] Sikorski A, Romiszowski P. Macromol Symp 2004;217:273.